of necessity be this putative intermediate(s). The lifetime of 11 or 11′ might be expected to be enhanced if it is in equilibrium with intermediate 10. This proposal is not unreasonable given the geometric constraints imposed on the system by the three-dimensional structure of DNA. Alternatively, 10 might be the long-lived intermediate that could undergo strand scission as an artifactual consequence of the method using ethidium bromide fluorescence changes to monitor strand scission.[25] Finally, Michael addition of H_2O to either 11 or 11′ would result in the production of 13 or 13′, respectively, which on the basis of recent studies of Sorensen and Jencks,[44] would rapidly be converted to the observed products 7 and 8 (Scheme II).

Summary. The following pieces of information must be accounted for in any mechanism proposed for base propenal formation by activated BLM: (1) the stereospecific removal of the 2′-*pro-R* proton; (2) the incorporation of one atom of ^{18}O into the carbonyl group of glycolic acid derived from the second O_2 equivalent; (3) the incorporation of ^{18}O from solvent into the aldehyde group of base propenal; (4) the 3′-C–O bond cleavage to generate a 5′-phosphate terminus; and (5) the kinetically more rapid release of the 2′-*pro-R* proton and DNA strand scission relative to the release of base propenal from DNA. While the traditionally accepted mechanism for base propenal formation (Scheme I, pathway A) meets the first four requirements, it cannot reconcile the kinetic uncoupling of 2′-*pro-R* proton release and strand scission from this process. The present studies, which have verified and expanded the observations of Burger et al.,[25] suggest that the putative "long-lived" precursor of base propenal is consistent with intermediate 10 in equilibrium with either 11 or 11′ (Scheme II).

DNA Binding and Photocleavage by Uranyl(VI) (UO₂²⁺) Salts

Peter E. Nielsen,*,§ Catharina Hiort,† Søren Holst Sönnichsen,§ Ole Buchardt,‡ Otto Dahl,‡ and Bengt Nordén†

Contribution from the Research Center for Medical Biotechnology, Department of Biochemistry B, University of Copenhagen, The Panum Institute, DK-2200 Copenhagen N, Denmark, Department of Physical Chemistry, Chalmers University of Technology, S-41296 Gothenburg, Sweden, and Research Center for Medical Biotechnology, Department of Organic Chemistry, The H.C. Ørsted Institute, University of Copenhagen, DK-2100 Copenhagen, Ø, Denmark.

Abstract: The interaction of the uranyl(VI) ion (UO₂²⁺) with DNA and its light-induced cleavage of DNA has been studied using flow-linear dichroism and ³²P-endlabeled oligonucleotides. It was found that binding of uranyl ion to DNA is a prerequisite for photocleavage; from run-off experiments the binding constant was estimated to be of the order of 10^{10} M⁻¹ at pH 4. The angular orientation of the [O=U=O]²⁺ chromophore is consistent with binding by bridging phosphate groups on opposite strands of the minor groove of DNA; at higher DNA concentration aggregation indicates intermolecular bridging as well. The uranyl-mediated photocleavage of DNA is not influenced by the presence of O_2, is more efficient at low pH (<7), and is virtually absent at pH 8.5. Subsequent treatment of uranyl photocleaved DNA with hot piperidine does not significantly increase the cleavage. The free nucleobases (adenine, cytosine, guanine, and thymine) were the major ethanol-soluble products to be observed after uranyl photocleavage of calf thymus DNA. From experiments using ³²P-endlabeled and methyl-phosphonate-containing oligonucleotides, it was concluded that upon irradiation attack by the uranyl ion occurs next to the phosphate to which it is bound, with equal preference for the 3′- and 5′-deoxyribose.

Introduction

Analysis of the structure and conformation of DNA complexes relies heavily on the employment of small probes that react with DNA either by forming covalent adducts or by inducing DNA strand scissions. These probes include alkylating agents, such as dimethyl sulfate (which primarily methylates N7 of guanine) or ethylnitrosourea (which ethylates oxygen on the DNA phosphates) or cleaving reagents such as EDTA/Fe(II) and various phenanthroline and bipyridyl complexes of transition metal ions (e.g., Cu(I), Ru(II), and Co(II)). The strand scission is typically caused by oxidation of the deoxyribose moiety of the DNA backbone.[1-5]

We have recently found that the uranyl(VI) ion (UO₂²⁺) induces single strand nicks in DNA upon irradiation with long wavelength ultraviolet light[6] which can be exploited for photo-footprinting of phosphate backbone contacts in protein–DNA complexes such as λ-repressor/O_R1,[6] *Escherichia coli* RNA polymerase/promoter,[7] and transcription factor IIIA-ICR interaction.[8] The uranyl ion, furthermore, serves as a sensitive probe of DNA conformation as exemplified in the modulation of the photocleavage of bent DNA and various other DNA sequences.[9,10]

Because of the potential of the uranyl ion mediated DNA photocleavage in molecular biology for studying DNA ligand complexes and DNA conformations it is important to understand the interaction of the uranyl ion, UO₂²⁺, with DNA.

The dynamic behavior of the uranyl/DNA system in the dark, its pH, and ionic strength dependencies as well as the photoinduced reactions resulting in DNA cleavage are complex. Previous studies[11] exploiting uranyl staining of DNA for electron microscopy have concluded that at low pH (<3.5) one uranyl ion is bound for every two phosphates of the DNA with an association constant

* To whom correspondence should be addressed.
† Chalmers University of Technology.
‡ University of Copenhagen.
§ The Panum Institute.

(1) Dervan, P. B. *Science* **1986**, *232*, 464–471.
(2) Sigman, D. S. *Acc. Chem. Res.* **1986**, *19*, 180–186.
(3) Tullius, T. D. *Ann. Rev. Biophys. Biophys. Chem.* **1989**, *1*, 213–237.
(4) Barton, J. *Science* **1986**, *233*, 727–734.
(5) Nielsen, P. E. *J. Mol. Recog.* **1990**, *3*, 1–25.
(6) Nielsen, P. E.; Jeppesen, C.; Buchardt, O. *FEBS Lett.* **1988**, *235*, 122–124.
(7) Jeppesen, C.; Nielsen, P. E. *Nucl. Acids Res.* **1989**, *17*, 4947–4956.
(8) Nielsen, P. E.; Jeppesen, C. *Trends Photochem. Photobiol.* **1990**, *1*, 39–47.
(9) Nielsen, P. E.; Møllegaard, N. E.; Jeppesen, C. *Anti Cancer Drug Design* **1990**, *5*, 105–110.
(10) Nielsen, P. E.; Møllegaard, N. E.; Jeppesen, C. *Nucl. Acids Res.* **1990**, *18*, 3847–3851.
(11) Zobel, C. R.; Beer, M. *J. Biophys. Biochem. Cyt.* **1961**, *10*, 335–346.

of 8×10^6 M^{-1}. At higher pH the ratio of uranyl/phosphate is ill defined presumably due to the formation of polynuclear uranyl complexes.[11] We have used a combination of chemical, biochemical, and spectroscopic techniques: polyacrylamide gel electrophoresis, chromatography, and phase-modulation flow linear dichroism to study the interaction of uranyl with DNA. The latter technique allows in situ probing of the transition moment orientation of flow-oriented DNA molecules and of indirectly oriented, associated ligands and can provide information about the hydrodynamic and spectroscopic properties of the DNA. These properties may be followed as a function of time using rapid phase-modulation signal analysis. The hydrodynamic part includes dependence on the contour length of DNA, the presence of flexible points and kinks, and the overall effect on persistence length from counter-ion charge shielding of the phosphate backbone; it is also a sensitive indicator of any formation of supercoils, compact particles, or aggregates. The spectroscopic part, furthermore, gives information about the secondary structure of the DNA (inclination of DNA bases) and about the binding geometry of any complexes that may be formed with chromophoric ligands.

The uranyl-mediated photocleavage of DNA was studied using a plasmid nicking assay, high resolution gel electrophoresis of 5'-^{32}P-endlabeled oligonucleotides, by which the sequence dependence of the photocleavage is analyzed, and by HPLC product analysis. Furthermore, the effect of substitutions (methylphosphonates and phosphorodithioates) in the DNA phosphate backbone of the oligonucleotides was examined.

Materials and Methods

Chemicals. Uranyl acetate dihydrate, purchased from Riedel-de-Haen, AG, was of analytical grade. The uranyl salt was dissolved in water acidified to pH $\sim$ 2, 4, or 7 with HCl. Alternatively, uranyl nitrate dissolved in H_2O (100 mM) was used. Citrate was purchased from KEBO Lab AB, Sweden, or Sigma (analytical grade). Calf thymus DNA was obtained from Sigma and used without further purification. The nucleotide concentration was determined spectroscopically using ϵ_{258} = 6600 M^{-1} cm^{-1}.[12] All linear dichroism experiments were carried out in Millipore water containing 10 mM sodium chloride.

Linear Dichroism. Linear dichroism, LD, is the differential absorption of orthogonal forms of linearly polarized light, defined as

$$LD = A_{\parallel} - A_{\perp} \qquad (1)$$

where $\parallel$ and $\perp$ denote, respectively, that the electric field vector of the light is parallel and perpendicular to the macroscopic orientation direction (in this case the flow direction). An oriented sample is thus a prerequisite for a nonvanishing LD. DNA solutions were oriented in a cell consisting of a rotating and a static cylinder, a so-called Couette device, of a type originally designed by Wada and Kozawa,[13,14] and LD was measured as described elsewhere.[15] A constant shear gradient of 1800 s^{-1} was used for recording the LD spectra, and the baseline was taken as the spectrum recorded at zero gradient.

For structural considerations it is convenient to use the reduced linear dichroism, LD^r,

$$LD^r(\lambda) = LD(\lambda)/A_{iso}(\lambda) \qquad (2)$$

where A_{iso} denotes the absorbance of the isotropic sample (the solution at rest). The reduced linear dichroism is related to molecular properties through the equation[16]

$$LD^r = \frac{3}{2} \cdot S \cdot (3\langle \cos^2 \alpha \rangle - 1) \qquad (3)$$

where α is the angle between the light absorbing transition moment

and the (local) DNA helix axis and $\langle \cos \rangle$ is an ensemble average over the different chromophores (or ligand sites). S is an orientation factor (for definition, see e.g., ref 16) which is a measure of the degree of alignment of DNA helices in the sample. For perfect orientation of DNA parallel to the flow direction S = 1 and for random orientation S = 0. For each uranyl-DNA sample the value of S was determined directly from the linear dichroism displayed in the DNA absorption band at 258 nm (using eq 3) and an effective angle of 86°, i.e., B-form DNA.[17-19] The assumption of a retained B-form is supported by the observation of a largely unchanged LD profile, consistent with an approximately wavelength independent LD^r as expected for the B-form.[19] Once S, the orientation of the DNA helix, has been determined, the measured LD^r at the wavelength (300-330 nm) of the uranyl chromophore can be interpreted in terms of a binding geometry characterized by the angle between the helix axis and the light absorbing transition in uranyl (through reuse of eq 3).

Binding Constant. The magnitude of the binding constant of the uranyl-DNA complex can be estimated by considering competing reactions:

$$DNA + UO_2^{2+} \underset{k_{-1}}{\overset{k_1}{\rightleftharpoons}} DNA{-}UO_2^{2+} \qquad (4)$$

$$UO_2^{2+} + citrate \underset{k_{-2}}{\overset{k_2}{\rightleftharpoons}} UO_2^{2+}{-}citrate \qquad (5)$$
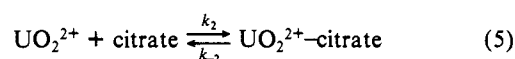
Compared to the other rate constants k_2 is large (the stability constant of the UO_2^{2+}-citrate complex is of the order of 10^8-10^9 M^{-1} [20]), and we may therefore apply the steady-state approximation to the treatment of the free uranyl ion. This is for very short times

$$\frac{d[DNA{-}UO_2^{2+}]}{dt} = -k_{-1} \cdot [DNA{-}UO_2^{2+}]$$

i.e., after introducing the binding ratio, r = $[DNA{-}UO_2^{2+}]/D_0$, where D_0 is the total concentration of DNA phosphate

$$\frac{dr}{dt} = -k_{-1} r$$

that is, in integrated form

$$\ln \{r\} - \ln\{r_{max}\} = -k_{-1} t \qquad (6)$$

where r_{max} denotes the uranyl binding ratio at t = 0 (where LD = 0), i.e., before citrate has been added. The virtually linear relationship between r and the measured LD (see Figure 2) can be expressed as LD = $(r_{max} - r) \cdot d$, where d is a scale factor given by the LD for r = 0 (pure DNA). In the experiment of Figure 6, r_{max} = 0.625 (assuming all uranyl is bound). At short times the equation

$$\ln \{r_{max} - LD/d\} - \ln r_{max} = -k_{-1} t \qquad (7)$$

then allows k_{-1} to be determined. The uranyl-DNA binding constant is estimated as k_1/k_{-1} on the assumption of a diffusion controlled run-on rate constant, k_1, of the order of 3×10^7 M^{-1} s^{-1}.[21]

Irradiation. The irradiation in the LD experiments was performed with the sample contained in a quartz cuvette with 1-cm path length. The light source, a Varian 450 W xenon lamp, was placed in line with a water container (light path $\sim$ 2 cm), to avoid heating of the sample with infrared light, and a Schott long pass filter cutting below 400 nm (transmittance = 0 at 400 nm, $\sim$85% above 470 nm). The sample cuvette was placed immediately after the filter.

Irradiation in all other experiments was performed with a Philips TL 40 W/03 fluorescent light tube emitting at 420 nm (20-nm band width, $\sim$20 J·m^{-2}·s^{-1}) or a Philips TL 20W/12 fluorescent light tube emitting at 300 nm (20-nm band width, $\sim$24 J·m^{-2}·s^{-1}).

(12) Mahler, H. R.; Kline, B.; Mehrota, B. D. *J. Mol. Biol.* **1964**, 9, 801.
(13) Wada, A.; Kozawa, S. *J. Polym. Sci. Part A* **1964**, 2, 853–864.
(14) Nordèn, B.; Tjerneld, F. *Biophys. Chem.* **1976**, 4, 191–198.
(15) Davidsson, Å.; Nordèn, B. *Chem. Scr.* **1976**, 9, 49–53.
(16) Nordèn, B. *Appl. Spectrosc. Rev.* **1978**, 14, 157–248.

(17) Arnott, S.; Dover, S. D.; Wonacott, A. J. *Acta Crystallogr., Sect. B: Struct. Crystallogr. Cryst. Chem.* **1969**, B25, 2192–2206.
(18) Matsouka, Y.; Nordèn, B. *Biopolymers* **1982**, 21, 2433–2452.
(19) Matsouka, Y.; Nordèn, B. *Biopolymers* **1983**, 22, 1731–1746.
(20) Rajan, K. S.; Martell, A. E. *Inorg. Chem.* **1965**, 4, 462–469.
(21) Langaa, P.; Markovits, J.; Delbarre, A.; Le Pecq, J.-B.; Roques, B. P. *Biochemistry* **1985**, 24, 5367–5575.

Plasmid Relaxation. A typical reaction mixture contained 0.5 μg of plasmid (pUC19) in 10 μL of buffer, 1.5 mM uranyl nitrate (diluted from a 100 mM stock solution), and the components indicated in Table III. The samples were irradiated from above (20-cm distance from the fluorescent light tube) in microfuge tubes. Irradiations in O$_2$ (or N$_2$) saturated solution and O$_2$ (or N$_2$) atmosphere were done by filling the microfuge tube with O$_2$ (or N$_2$), equilibrating by whirly mixing three times within 5 min (this was repeated three times) and finally covering the tube with polyethylene film during the irradiation. The samples were analyzed by gel electrophoresis in 1% agarose, 0.5 $\times$ TBE buffer (TBE = 90 mM Tris-borate, pH 8.3, 1 mM EDTA), and the gels were stained with ethidium bromide and photographed. Quantification was performed by densitometric scanning of the photographs.

Quantum Yield Calculation. The quantum yield of the uranyl mediated photocleavage of plasmid DNA was calculated using results obtained in sodium acetate buffer and using 300-nm radiation: At a UO$_2^{2+}$ concentration of 10 μM and a plasmid DNA (2686 base pairs) concentration of 90 μM (in base pairs) in 10 μL of 50 mM sodium acetate buffer, pH 6.3, 50% nicking was achieved with 30 min irradiation. The light intensity was measured as 24 J$\cdot$m^{-2}$\cdot$s^{-1} (by phenylglyoxal actinometry using the same sample set-up as for the uranyl photocleavage experiments), corresponding to 4.4 $\times$ 10^{15} quanta$\cdot$s^{-1}$\cdot$cm^{-2} at 300 nm. Since the area of the irradiated sample was 0.12 cm^2, the total radiation flux during 30 min was 9.5 $\times$ 10^{17} quanta.

The extinction coefficient of the UO$_2^{2+}$ in acetate buffer was determined as 1140 M^{-1} cm^{-1} at 300 nm, which means that the absorbance of the sample (10 μM UO$_2^{2+}$ and a light path of 0.1 cm) was 1.14 $\times$ 10^{-3}. Thus 1.1 $\times$ 10^{15} light quanta were absorbed. The number of strand breaks can be calculated as 90 μM $\times$ 1/5372 $\times$ 10 μL$\cdot$6 $\times$ 10^{23} M^{-1} = 10^{11} breaks. This leads to a quantum yield for the uranyl-mediated photonicking of plasmid DNA in 50 mM sodium acetate, pH 6.3 at 300 nm of 10^{11}/(1.1 $\times$ 10^{15}) = 10^{-4} nicks/absorbed light quantum.

Oligonucleotide Synthesis and Analysis. Oligonucleotides were synthesized by standard phosphoramidite chemistry on a Biosearch 7500 DNA synthesizer. Methylphosphonate linkages were introduced by substitution of phosphoramidites with methylphosphonamidites and the phosphorodithioate linkage by substitution with *O*-(5'-*O*-(dimethoxytrityl)-*N*-benzoyl-2'-deoxy-cytidine-3'-yl)-*S*-(2-cyanoethyl)-*N*,*N*-(dimethylthio)phosphoramidite, prepared in the same way as the analogous thymidine derivative.[22] In the latter case the coupling was performed manually for 5 min and was followed immediately by treatment with sulfur (1.5 M in pyridine/CS$_2$, 1:1, 6 min). The products were purified by ethanol precipitation and labeled with ^{32}P-γATP (Amersham, 3000 Ci/mmol) at the 5'-end by standard techniques[23] using T$_4$ polynucleotide kinase (Gibco-BRL).

Uranyl-mediated photocleavage was performed in 100 μL of H$_2$O containing 0.5 μg of calf thymus DNA, ~30 000 cpm 5'-^{32}P-endlabeled oligonucleotide, 150 μM or 1 mM of uranyl nitrate, and the desired buffer components. Irradiations were performed in microfuge tubes at 420 nm. The DNA was precipitated with 250 μL of ethanol after addition of 20 μL of 0.5 M sodium acetate, pH 4.5 (the low pH prevents co-precipitation of uranyl, which interferes with subsequent gel electrophoretic analysis) and was analyzed by electrophoresis in 20% polyacrylamide, 7 M urea TBE sequencing gels.[23] Radioactive DNA fragments were visualized by autoradiography (Agfa curix RP1 X-ray film) at −70 °C for 12–24 h using intensifying screens. The autoradiograms were scanned at 550 nm using a Shimadzu CS930 densitometric scanner equipped with a DR2 recorder.

HPLC Analysis. A solution (100 μL) of calf thymus DNA (1 mM phosphate) in 50 mM ammonium acetate, pH 6.5, 1 mM uranyl nitrate was irradiated from above in a microfuge tube

(22) Dahl, B. H.; Bjergårde, K.; Sommer, V. B.; Dahl, O. *Acta Chem. Scand.* **1989**, *43*, 896–901.
(23) Maniatis, T.; Fritsch, E. F.; Sambrook, J. *Molecular Cloning. A Laboratory Manual*; Cold Spring Harbor Laboratory Press: 1982.
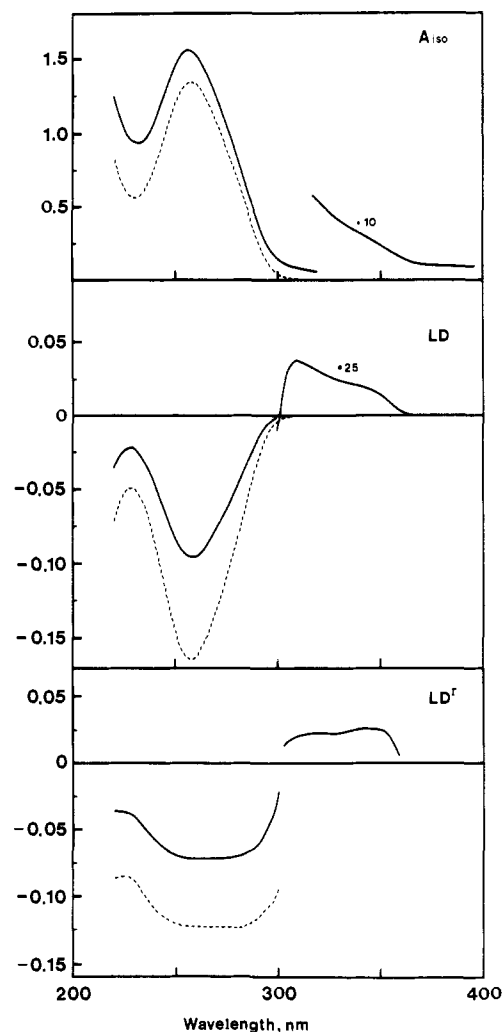
Figure 1. Normal absorption (A_{iso}), linear dichroism (LD), and reduced linear dichroism (LD^r) of uranyl in the presence of calf thymus DNA. The total concentrations of uranyl (U$_0$) and DNA (D$_0$) were 100 and 250 μM, respectively. The spectra were recorded at pH 4. Broken curves show the spectra of pure DNA. A_{iso} and LD are given in absorbance units.

(covered with polyethylene film) at 420 nm (Philips TL 40W/03 fluorescent light tube), and the DNA was subsequently precipitated with 500 μL of ethanol at −50 °C. The supernatant (10.000 g, 20 min) was lyophilized, redissolved in 50 μL of 50 mM KH$_2$PO$_4$, pH 3.5, and analyzed by HPLC using a reversed phase C$_{18}$ column and a Spectra Physics/Spectra Focus SP8800 instrument. The eluant was 50 mM potassium phosphate, pH 3.5, 5% methanol, 1% acetonitrile, and 0.2% tetrahydrofuran. Peaks were monitored at 190–350 nmn.

Results

Linear Dichroism. Figure 1 shows representative A_{iso}, LD, and LD^r spectra for calf thymus DNA samples in the presence of uranyl acetate. That uranyl displays flow linear dichroism is irrefutable evidence for complexation of uranyl to DNA, since LD is nonzero only for oriented species, in this case DNA and the uranyl bound to it. The observed decrease in LD amplitude for the DNA band, upon addition of uranyl, is additional evidence for the uranyl–DNA interaction. Unfortunately, the LD of the uranyl absorption band around 320 nm is detectable only for a very narrow range of uranyl and DNA concentrations, pH, and ionic strengths. However, the observed change in DNA LD can be used to monitor the interaction of uranyl with DNA indirectly under biologically relevant conditions.

Linear Dichroism of the Uranyl Absorption. Figure 1 shows that flow oriented DNA displays a weak structured LD band in its UV-absorption region (below 340 nm) upon interaction with
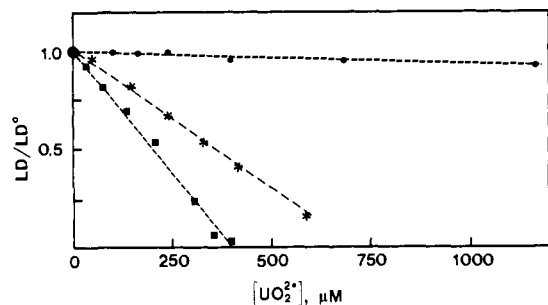
Figure 2. Ratio between LD (the linear dichroism of the uranyl–DNA samples) and LD^0 (LD of pure DNA) as a function of total uranyl concentration. Circles, stars, and squares denote pH 7, 4, and 2 in the uranyl stock solutions, respectively. LD was measured at 258 nm.

uranyl. The uranyl LD is partly overlapped by the DNA signal. Since the extinction coefficient of uranyl in the visible region is only ∼20 M^{-1} cm^{-1}, its LD could not be detected in the long wavelength part of the spectrum.

In order to determine the binding geometry of the uranyl DNA complex, we calculated the reduced linear dichroism for the uranyl absorption band at 320 nm where DNA displays no LD (in Figure 1, LD^r(uranyl) = +0.022). Applying eq 3 (and using S = 0.049 obtained from LD^r (DNA) = −0.072 in the DNA absorption region) we concluded that the uranyl transition at 320 nm is polarized at an angle approximately 49° to the DNA helix axis. From symmetry and molecular orbital arguments, it is inferred that the moment of the first strong transition of uranyl is parallel to the O=U=O axis. An angle of 49° is identical with the pitch of the phosphate backbone and is consistent with the long axis of uranyl being parallel to the inclination of either groove. This orientation would agree well with interaction between the equatorial coordination positions of uranyl and oxygens of the DNA phosphates on both sides of the groove. When measuring the LD^r of uranyl samples at different pH values (4.5 and 6) and DNA-phosphate concentrations (0.25 and 0.4 mM), α was again found to be 49 ± 2°. This observation demonstrates that the factors leading to decreased linear dichroism, e.g., aggregation and condensation (vide infra), do not significantly influence the (microscopic) uranyl binding geometry but only the value of the (macroscopic) orientation factor.

Linear Dichroism of the DNA Absorption. Figure 2 shows that the LD in the DNA band decreases significantly upon addition of uranyl, and it vanishes completely at high uranyl/DNA ratios. However, the shape of the band is virtually unchanged throughout the titration. This demonstrates that the contribution from uranyl to the LD in this region is negligible since there would be changes in the spectral proportions if uranyl had contributed. Consequently, the decrease in LD at 260 nm can be attributed solely to a corresponding decrease in the average orientation of DNA induced by the interaction with uranyl.

There are two possible explanations for the observed decrease in the DNA orientation in the presence of uranyl: (i) intermolecular bridging (formation of aggregates) and (ii) intramolecular perturbations (condensation or kink formation). In order to discriminate between these effects, we performed LD measurements at identical uranyl/DNA ratios but varying DNA concentrations. Figure 3 shows that the orientation decreases more for a given binding ratio at high DNA concentrations, indicating that the presence of uranyl leads to some aggregation. Such aggregation can be explained by intermolecular DNA bridging in accord with the reported ability of uranyl to form polyligand and also polynuclear complexes with inorganic phosphate.[24]

The ratio of LD/LD^0 (LD^0 denotes the LD of pure DNA at pH 7 and 10 mM NaCl) depends significantly on the pH of the added uranyl stock solution (Figure 2). At 350 μM uranyl, for example, the LD/LD^0 is close to unity for pH 7, whereas the ratio is only 0.1 in a sample where pH is 4. This marked pH dependency
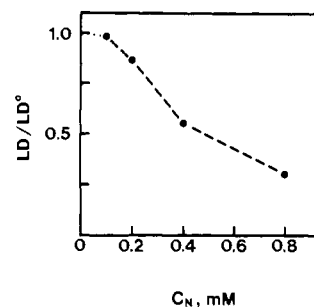
Figure 3. DNA orientation as a function of DNA phosphate concentration in the presence of uranyl. The ratio $[UO_2^{2+}]$/DNA was kept constant and was equal to 0.6. LD^0 is the LD of pure DNA prior to uranyl (pH 4) addition. LD was measured at 258 nm.
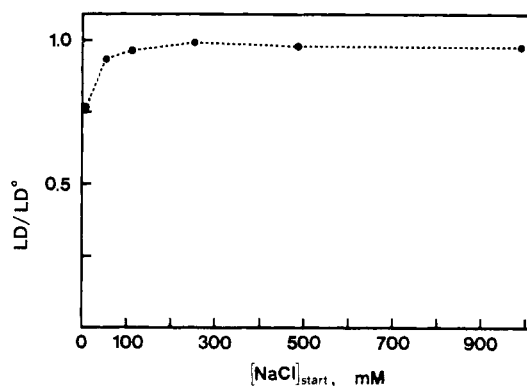
Figure 4. LD/LD^0 versus sodium chloride concentration present in the sample before adding uranyl. LD^0 is the LD of pure DNA at each NaCl concentration. $[UO_2^{2+}]$ = 100 μM, [DNA] = 400 μM. pH was 2 in the uranyl stock solution. LD was measured at 258 nm.

cannot be explained by the change of pH alone, since the orientation of pure DNA is essentially independent of pH between pH 4 and 7.[25] The less pronounced decrease in DNA LD for the higher pH values in the examined range can be explained by the tendency of uranyl to form strong complexes with hydroxide ions.[26,27] Such positive or uncharged complexes will have low affinity for DNA and consequently the binding ratio of uranyl to DNA decreases with increasing pH.

The uranyl-induced decrease in DNA LD is not reversed by the addition of up to 1 M NaCl, in support of a very strong binding of uranyl to DNA. On the other hand, if the order of adding uranyl and salt is reversed so that uranyl is added to a sample containing sodium chloride, the decrease in LD is noticeably smaller and, for high salt concentration, almost negligible (Figure 4). This observation suggests that shielding of the negative phosphate charges by the sodium ion cloud significantly diminishes the attraction between DNA and uranyl, preventing primary (electrostatic) association and reaction into the final, strong complex. As a result the orientation is less affected in this case.

It is difficult to use LD to study how divalent cations affect the uranyl binding to DNA, as most divalent cations associate strongly to DNA and thereby affect the orientation significantly. Citrate, however, a strong, anionic metal-ion chelator with no intrinsic effect on DNA, is found to restore the DNA orientation almost completely (Figure 5). The amplitude of the negative LD signal increased for a long period (>5 h) after citrate was added showing that the complete displacement of uranyl from DNA (the run-off rate) is very slow. If the citrate concentration is high, approximately 100% of the original DNA LD signal is recovered. The kinetics of the LD recovery is consistent with a binding constant for uranyl to DNA of the order of 10^9–10^{10} M^{-1} at pH 4 (Figure 5) if one assumes a diffusion-controlled run-on rate

(24) Smith, R. M.; Martell, A. E. *Critical Stability Constants. Inorganic Complexes*; Plenum Press: New York and London, 1976; Vol. 4.

(25) Nordén, B.; Seth, S. *Biopolymers* **1979**, *18*, 2323–2339.
(26) Schreyer, J. M.; Baes, C. F., Jr. *J. Am. Chem. Soc.* **1954**, *76*, 354–357.
(27) Greenwood, N. N.; Earnshaw, A. *Chemistry of the Elements*; Pergamon Press: Oxford, 1986; p 1478.
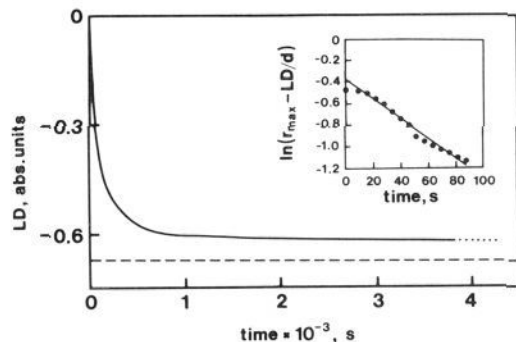
Figure 5. LD versus time. At $t = 0$, citrate was added to a uranyl–DNA sample with LD = 0. The total citrate concentration was 1 mM [UO₂²⁺] = 250 μM, [DNA] = 400 μM. pH was 4 in the final solution. LD was measured at 258 nm. Inset: plot of eq 17 for the experiment above is shown. The slope, representing the off-rate constant k_1, is 0.008 s⁻¹.
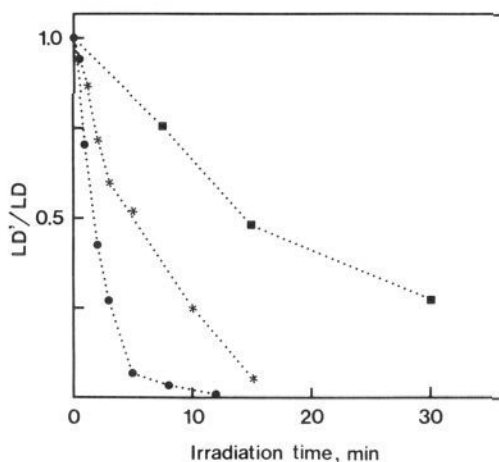
Figure 6. Ratio between LD′ (for the irradiated uranyl–DNA samples) and LD (before irradiation) versus irradiation time. Squares, stars, and circles represent pH 7, 4, and 2 in the uranyl stock solutions, respectively. [DNA] ≈ 400 μM, [UO₂²⁺] = 100 μM. LD was measured at 258 nm.

Figure 7. Uranyl photocleavage of 5′-³²P-endlabeled oligonucleotide. All samples contained 30.000 cpm ³²P-44 mer oligonucleotide: 5′-AATTCGTACCTAGGTCTACCGTGCCGGATCCCGGGTA and 0.5 μg calf thymus DNA in 100 μL of 50 mM buffer. All samples except 1 (no uranyl control) contained 1 mM UO₂(NO₃)₂, and all samples except 2 (no light control) were irradiated at 420 nm for 30 min. The following buffers were used: lanes 3–8, Tris-HCl, pH 7.0; lanes 9–11, Tris-HCl, pH 6.5, 7.5, or 8.5, respectively; lane 12, sodium acetate, pH 6.5, lane 13, sodium phosphate, pH 7.0. Sample 3 was irradiated at 0 °C, sample 5 at 40 °C, and all other samples at 20 °C. Sample 6 was saturated with O₂ and irradiated in an O₂ atmosphere, while sample 7 was saturated with N₂ and irradiated in an N₂ atmosphere. Sample 8 was treated with 1 M piperidine at 90 °C (20 min) prior to electrophoresis. Lane S is an A/G sequence marker produced by formic acid/piperidine treatment according to the Maxam–Gilbert sequencing protecol.

similar to that observed with intercalators.[21]

Linear Dichroism of DNA After Irradiation. Upon irradiation of the uranyl–DNA sample, the LD decreases further (Figure 6). We ascribe this decrease to the increased flexibility of the DNA helix as a result of the photonicking of DNA by uranyl.[6] The DNA orientation, and hence the LD signal, is strongly dependent on the persistence length of DNA and should be diminished significantly by the increased flexibility of the double helix at the point of strand breakage. The cleavage efficiency clearly increases with decreasing pH between pH 7 and 2. This is consistent with an increased uranyl/DNA binding ratio as pH is lowered (cf. Figure 2). The photonicking is inhibited by citrate (results not shown) confirming that binding of the uranyl to the DNA is a prerequisite for photocleavage.

Photocleavage of Oligonucleotides. 5′-³²P-endlabeled oligonucleotides were used to examine the influence of temperature, oxygen and pH on the uranyl-mediated photocleavage of DNA. As shown in Figure 7 neither the temperature (0–40 °C) nor saturation of the medium with O₂ (or N₂) have any significant effect on the photocleavage (lanes 3–7). However, the photocleavage is dramatically decreased with increasing pH (pH 6.5–8.5, lanes 9–11). Treatment of uranyl photocleaved oligonucleotide with piperidine at 90 °C results in only a marginally increased cleavage (10–20%) especially at thymine residues. Finally, photocleavage is reduced in acetate buffer (lane 12) and is virtually absent in phosphate buffer (lane 13). It is also seen that the major photocleavage products comigrate with those of the Maxam–Gilbert sequencing reaction, i.e., they migrate as 3′-phosphates. This is consistent with previous results showing that uranyl photocleavage of endlabeled double stranded DNA fragments

predominantly gives rise to single bands when analyzed by polyacrylamide gel electrophoresis, one band corresponding to each base position.[6,7] These bands comigrate with the bands obtained by chemical DNA sequencing,[6,7] i.e., they correspond to the 3′- and 5′-phosphates. Thus uranyl photocleavage of DNA predominantly removes nucleoside units (deoxyribose + base) (some minor cleavage products migrating in between the 3′-phosphates are also observed).

In order to examine the relation between uranyl phosphate binding and DNA cleavage directly, we studied the uranyl photoinduced cleavage of $5'$-^{32}P-endlabeled oligonucleotides containing methylphosphonates at specific positions. Upon gel analysis (Figure 8) of the products from uranyl-mediated photocleavage of these oligonucleotides it is observed that the intensities of two bands are specifically reduced. These bands correspond to cleavage at either side of the methylphosphonate, and the results therefore show that photooxidation of the deoxyribose on either side of the methylphosphonate (bands marked with arrowheads in Figure 8, lanes 5, 6, and 15) is significantly reduced (more than 50%, Figure 9b). Inclusion of two adjacent methylphosphonates similarly results in highly reduced photocleavage at three positions (Figure 8, lane 14, Figure 9c). These experiments were performed at low uranyl concentrations (50 μM). At higher concentrations of uranyl ($\sim$1 mM) the discrimination between phosphates and methylphosphonates is much less pronounced[28] (results not shown), indicating that uranyl does have some affinity for methylphosphonates (maybe by bridging to a neighboring phosphate). This probably also explains why some photocleavage takes place at the deoxyribose between the two methylphosphonates (Figure 9c).

Photocleavage of a 20-mer oligonucleotide containing a single dithioate (S=P—S$^-$) in place of a phosphate results in a highly increased ($\sim$10-fold) uranyl photocleavage at this position (Figure 8, lane 10). This photocleavage also occurs in the presence of EDTA or citrate (Figure 8, lanes 11 and 12) where cleavage at phosphate linkages is not observed. These results show that uranyl has higher affinity for phosphorodithioates than for phosphate. The nature of this cleavage is not known, but we note that it results in one major cleavage site, and that the band from this cleavage does not comigrate with a $3'$-phosphate. These results show that the uranyl-mediated cleavage of DNA can be modulated by the nature of the "phosphate" linkages and directed to specifically modified sites.

Photocleavage of Calf Thymus DNA. Uranyl-mediated photocleavage of calf thymus DNA leads to liberation of four major ethanol soluble products in the ratio 6:3:3:1 (Figure 10). These were identified by HPLC as the four nucleobases, cytosine, adenine, thymine, and guanine on the basis of retention times, UV-spectra, and co-injection with authentic samples. The amount of liberated nucleobases increased linearly with irradiation time for at least 30 h. On the basis of the finding that uranyl-mediated DNA photocleavage is virtually nucleobase—and to a great extent also sequence-independent,[6,7] liberation of almost equal amounts of the four nucleobases could be anticipated (calf thymus DNA contains 56% AT), but some deviation from the nucleobase ratio present in calf thymus DNA is not unexpected since the photocleavage was performed in ammonium acetate buffer, and under these conditions a significant sequence modulation is observed.[10] However, this cannot account for the very low level of liberated guanine. Guanine is the most easily oxidized nucleobase,[29] and in a control experiment it was found that $\sim$70% of the guanine was degraded upon irradiating a mixture of adenine, cytosine, guanine, and thymine in the presence of uranyl under the conditions used for uranyl photocleavage of calf thymus DNA, whereas only little degradation of adenine and thymine (<10%) and no degradation of cytosine took place. No uranyl photooxidation of guanine in the DNA helix is likely to take place, however, since uranyl photocleavage of ^{32}P-endlabeled oligonucleotides does not lead to alkaline sensitive sites at guanine residues. We thus conclude that the low level of detectable guanine is due to oxidation of liberated guanine by uranyl.

In order to establish a link between DNA strand scission and base liberation, we performed a uranyl photocleavage experiment in which we measured both the cleavage of a ^{32}P-endlabeled

(28) Nielsen, P. E.; Cons, B.; Sommer, V. B.; Fox, K. In *Molecular Basis of Specificity in Nucleic Acid–Drug Interactions*; Pullman, B., Jortner, J., Eds.; The Jerusalem Symposium on Quantum Chemistry and Biochemistry; Kluwer Academic Publishers: 1990; Vol. *23*, pp 423–432.

(29) Jovanovic, S. V.; Simic, M. G. *Biochim. Biophys. Acta* **1989**, *1008*, 39–44.

Table I. Correlation between Strand Scission and Nucleobase Release

irradiation time (hours)[a]	2	4	6
% strand scission[b]	3	7	8
% nucleobase release[c]	2	8	10

[a] Each sample contained 4 μg oligonucleotide ($5'$-TCGAGA-GATCTGTACGTTAG) in 100 μL of 50 mM NH$_4$ acetate, pH 7.0, 1 mM UO$_2$(NO$_3$)$_2$ and was irradiated at 420 nm for the indicated times. [b] Determined by gel electrophoretic/autoradiographic measurement of remaining, intact oligonucleotide, assuming a Poisson distribution of the strand scissions. [c] Measured by HPLC using an aliquot of the sample used for gel electrophoresis. The results are averages of the release of all four (adenine, cytosine, guanine, and thymine) nucleobases.

Table II. Reaction of Uranyl–DNA Photoproducts with Thiobarbituric Acid (According to Ref 30)

reagent	DNA	radiation[a]	E_{532}
uranyl	–	+	0.00
uranyl	+	–	0.044
uranyl	+	+	0.059
bleomycin/Fe^{2+} [b]	+	–	1.93

[a] The uranyl sample was irradiated at 420 nm for 9 h. [b] The bleomycin sample was incubated at 20 °C for 30 min, which according to HPLC analysis released an amount of adenine comparable to that released by uranyl phototreatment in *a*. Control experiments showed that addition of uranyl to the bleomycin cleaved DNA did not affect the subsequent barbiturate reaction.

Table III. Uranyl-Mediated Photocleavage of Plasmid DNA[a]

buffer conditions[b]	pH	final pH[c]	sc[d]	r[d]	l[d]	nicks/DNA[e]
Tris-HCl	6.5	4.6	0	76	24	>10
	7.0	6.2	0	74	26	>10
	7.25	7.1	19	81	0	1.5
	7.5	7.4	45	55	0	0.85
	8.0	7.9	66	34	0	0.4
	8.5	8.5	80	20	0	0.2
sodium acetate	6.5	6.3	0	75	25	>10
Hepes	6.5	6.3	0	74	26	>10
	7.5	7.5	9	82	9	2.5
Pipes	6.5	6.5[f]	0	88	12	>10
	7.5	7.4[f]	30	70	0	1.2
potassium phosphate	6.5	6.8[g]	92	8	0	0.1
	7.5	7.4[g]	92	8	0	0.1
10 mM MgCl$_2$[h]			45	55	0	0.8
100 mM NaCl[h]			43	57	0	0.9
400 mM NaCl[h]			48	52	0	0.7
1 mM citrate[h]			36	64	0	1.05
2 mM citrate[h]			82	18	0	0.15
0.5 mM EDTA[h]			78	22	0	0.25
1 mM EDTA[h]			89	11	0	0.1
10% glycerol[h]			30	70	0	1.2
control[i]			90	10	0	0.1

[a] Each sample contained 0.5 μg of plasmid DNA and 1.5 mM uranyl nitrate (which was added last) in 10 μL of buffer. The samples were irradiated for 30 min at 420 nm. [b] The buffers were 50 mM. [c] pH measured in a solution of 50 mM buffer and 1.5 mM uranyl nitrate. [d] % supercoiled plasmid (sc), relaxed (nicked) plasmid (r), or linear plasmid (1), respectively. [e] Number of nicks per plasmid calculated from the amount of supercoiled DNA and assuming a Poisson distribution of the nicks. [f] Precipitation occurred. [g] Heavy precipitation occurred (uranyl phosphate). [h] This sample also contained 50 mM Tris-HCl, pH 7.5. [i] Not irradiated.

oligonucleotide by gel electrophoresis and the liberation of nucleobases by HPLC analysis. These results (Table I) are fully compatible with a mechanism resulting in the liberation of one nucleobase for every strand scission.

Four minor products were also detected by the HPLC analysis. These exhibited UV-spectra compatible with being nucleobase derived, e.g., in the form of nucleobases to which fragments of deoxyribose are still attached. We can rule out, however, that they are base propenals,[30] since the thiobarbiturate reaction was
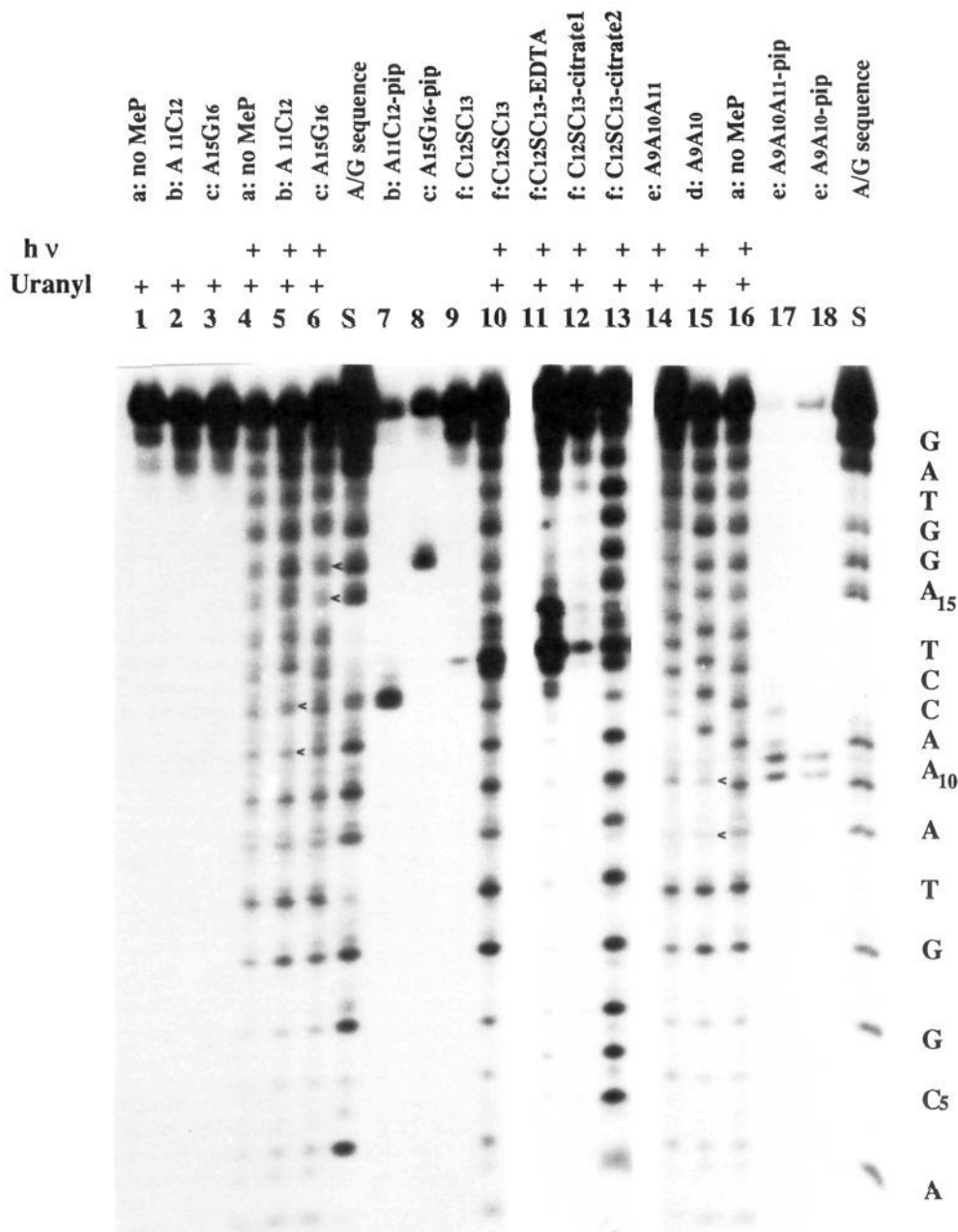
Figure 8. Gel electrophoretic analysis of uranyl mediated photocleavage (150 μM uranyl, 5 h irradiation) of methylphosphonate- or phosphorodithioate-containing oligonucleotides. The sequence of the 20-mer oligonucleotide was 5'-G$_1$GCACGGTAAACCTAGGTAG (a) with one methylphosphonate between positions A$_{11}$C$_{12}$ (b), A$_{15}$G$_{16}$ (c), or A$_9$A$_{10}$ (d), two methylphosphonates at positions A$_9$A$_{10}$A$_{11}$ (e), or a dithioate at position C$_{12}$C$_{13}$ (f). The 20-mers used were as follows: lanes 1, 4, and 16, a; lanes 2, 5, and 7, b; lanes 3, 6, and 8, c; lanes 9–13, f; lanes 14 and 17, e; lanes 15 and 18, d; lanes S are A+G sequencing reactions. The samples of lanes 1–3 and 9 were not irradiated, while those of lanes 4–6 and 14–16 were. The samples of lanes 7, 8, 17, and 18 are the 20-mers hydrolyzed by piperidine to verify the positions of the methylphosphonates. The samples of lanes 10–13 were irradiated for 30 min in the presence of 2 mM uranyl (lane 10), 2 mM uranyl + 1 mM EDTA (lane 11), 2 mM uranyl + 2 mM citrate (lane 12), or 2 mM uranyl + 1 mM citrate (lane 13). Since methylphosphonate containing oligonucleotides migrate slightly slower than unmodified oligonucleotides (the former has one negative charge less per methylphosphonate), comigration of cleavage products and the sequence marker are only observed for the shorter fragments which do not contain the methylphosphonate. This is easily seen when comparing lanes 14, 15, and 16.

negative for the uranyl–DNA photocleavage products (Table II).

Plasmid Relaxation. A plasmid relaxation assay was used to obtain quantifiable results of the effect of buffer, pH, and temperature on the uranyl-mediated photocleavage of DNA and to extend the findings obtained with single stranded oligonucleotides to double stranded DNA. The plasmid relaxation results (Table III) show that the efficiency of the uranyl-mediated photocleavage of double stranded DNA is strongly influenced by the medium. In accordance with the LD and the oligonucleotide results the

photocleavage is by far most efficient at low pH irrespective of the buffer employed. Phosphate buffer is an exception since no cleavage was detected even at pH 6.5. This is undoubtedly due to the formation of insoluble uranyl phosphates.[31] Indeed, a concentration dependent inhibition of the uranyl DNA photocleavage is observed when low concentrations of sodium phosphate (0–75 μM at 150 μM uranyl) is added in potassium acetate buffer pH 6.5 (results not shown).

Biologically relevant concentrations of Mg²⁺ (10 mM) or Na⁺ (100–400 mM) does not affect the cleavage. Both from a

(30) Burger, R. M.; Berkowitz, A. R.; Peisach, J.; Howitz, S. B. *J. Biol. Chem.* **1980**, *255*, 11832–11838.

(31) Karpow, V. I. *Zhur. Neorg. Khim.* **1961**, *6*, 531–532.

a

b

c
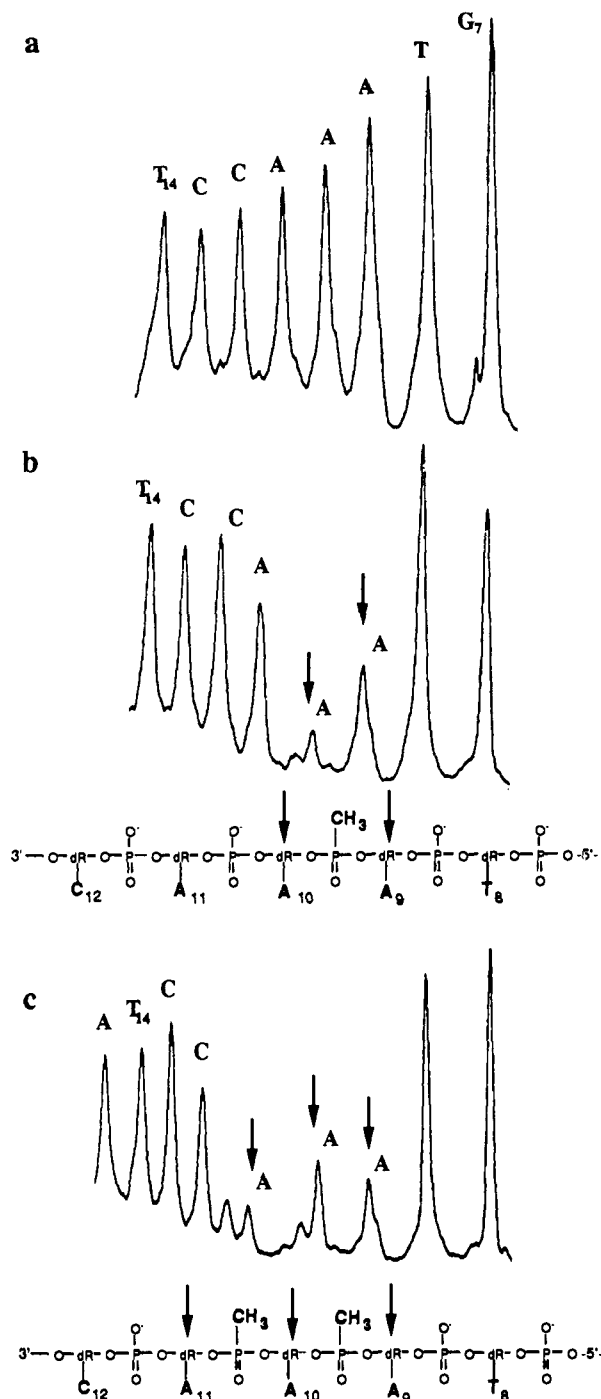
Figure 9. Densitometric scanning of an autoradiograph from an experiment as the one shown in Figure 8. The lanes corresponding to 16 (a, control), 15 (b, one methyl phosphonate between A_9A_{10} (20-mer-d), or 14 (c, two methylphosphonates at $A_9A_{10}A_{11}$ (20-mer-e)) were scanned at 550 nm. The bands at the arrow in b correspond to oxidation of the deoxyribose marked with an identical arrow in the formula. Comigration of oligonucleotide fragments are observed for G_7 and T_8 but not for C_{12}, C_{13}, T_{14}, etc., due to the presence of the methylphosphonate linkage at A_9A_{10} (and $A_{10}A_{11}$).

mechanistic and biological point of view it is interesting that the cleavage is not inhibited—in fact it is slightly enhanced—by the radical quencher glycerol (10%). Furthermore, equimolar concentrations of the metal ion chelators EDTA or citrate inhibits the uranyl-mediated DNA photocleavage. Varying the temperature within the biological range (0–40 °C) did not have any effect on the rate of uranyl-mediated DNA photocleavage and neither had the presence or absence of O_2/N_2 (results not shown).

Using the data from the photonicking of plasmid DNA in acetate buffer, the extinction coefficient of uranyl nitrate in this
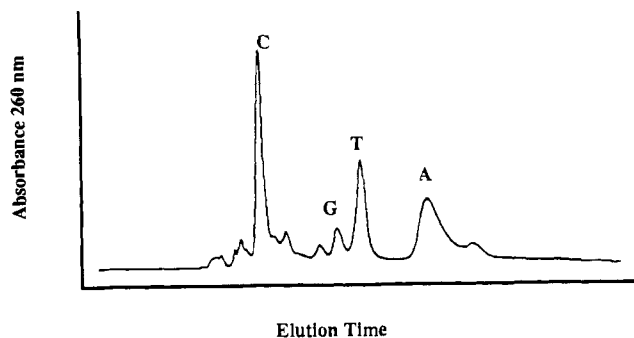
Elution Time

Figure 10. HPLC analysis of the ethanol soluble products from uranyl-mediated photocleavage of calf thymus DNA. The bases adenine (A), cytosine (C), guanine (G), and thymine (T) are marked based on retention times, UV spectra, and co-injection experiments. The trace was obtained from a sample after 24 h of irradiation, and the amounts of liberated nucleobases were calculated from the area of the peaks using the extinction coefficients of the nucleobases at 260 nm.

buffer and the intensity of the irradiation source, we can estimate a quantum yield for the uranyl-mediated DNA photocleavage of $\sim 10^{-4}$ nicks/uranyl·quantum. This number should be taken as a lower limit, since we do not know how much of the added uranyl is actually bound to the DNA and how much has formed inactive "hydroxides". The quantum yield was found to be independent on the irradiation wavelength (300 versus 420 nm), but due to the larger extinction coefficient at 300 nm the photocleavage is >10 fold more efficient at this wavelength. Finally, the quantum yield for liberation of nucleobases at 420 nm measured by HPLC analysis was also found to be $\sim 10^{-4}$ bases/uranyl·quantum.

Discussion

DNA Binding. It is well-known that solutions of UO_2^{2+} are only stable at low pH and that polynuclear uranyl complexes and "uranyl hydroxide" precipitates are formed at higher pH.[24,27] It is therefore not surprising that the interaction of UO_2^{2+} with DNA in the physiological pH range (pH 6–8) exhibits a rather complex behavior.

It has previously been shown by a precipitation assay that uranyl binds stoichiometrically well-defined to DNA with one uranyl per two phosphates at low pH (<3.5) and in a complex manner at higher pH.[11]

The present results clearly confirm that the uranyl(VI) ion binds strongly to DNA with an estimated affinity constant of 10^{10} M^{-1} at pH 4. This is considerably stronger than the binding of either Mg^{2+} or Na^+, and this estimate is approximately three orders of magnitude higher than that previously determined by precipitation. We believe that our estimate is more accurate since it is based on kinetic measurements. The uranyl–DNA complex formation is fully reversible, since a strong chelator like citrate efficiently removes uranyl from the DNA. In view of these findings, it may seem inconsistent that uranyl binds less efficiently to DNA in the presence of Na^+. This is ascribed to a kinetic effect. In the presence of Na^+ (or Mg^{2+}), shielding the negative charges of the DNA phosphate backbone, the kinetics of the uranyl–DNA association is slowed down and thus competing reactions—uranyl polynuclear complex formation and precipitation—decrease the amount of productive DNA-binding and DNA-photocleaving species. The higher efficiency of the uranyl–DNA association at lower pH (pH 2–6) is interpreted in a similar way; at lower pH unproductive competing reactions proceed more slowly than at higher pH. The pH dependence of the binding of uranyl to DNA also explains the analogous pH dependence of the photocleavage (Table III). This also means that when uranyl is used for biological experiments employing buffers at pH 6–7, we are working with a metastable system relying on the fast kinetics of uranyl–DNA binding combined with the long half-life of this complex.

Although we have estimated the affinity of the UO_2^{2+} ion for DNA indirectly, we are confident that our estimate is fairly accurate. The uranyl–citrate complexation constant has been

Uranyl(VI) (UO₂²⁺) Salts

J. Am. Chem. Soc., Vol. 114, No. 13, 1992 4975

determined as 10^8–10^9 M^{-1} (dependent on the ligand concentrations) at pH 2–4 where predominantly bimolecular uranyl–citrate complexes are formed[20] (at higher pH polymeric complexes are formed). The observation that it requires 2 mM citrate to inhibit the uranyl-mediated DNA photocleavage (Table III) at ∼1.6 mM DNA (calculated as phosphates) indicates that the affinity of UO_2^{2+} for DNA is slightly higher than that for citrate. Since we could not measure the uranyl DNA binding at higher pH (in the physiological range), and the affinity of citrate for uranyl is not known at higher pH either, we cannot say if this high stability of the uranyl–DNA complex also prevails at higher pH. However, as stated above, we are dealing with a highly complex metastable system and therefore a description involving a single binding constant is hardly adequate but can be viewed as a guideline.

Our observations on the UO_2^{2+}–DNA complex do not conclusively determine the binding mode, but the flow linear dichroism data suggest that the UO_2^{2+} (at least at low pH) is bound in either or both of the DNA grooves, possibly bridging the phosphates across the groove. A bridging mechanism would favor minor groove binding, since X-ray data on uranyl salts show that the ligand–ligand distance (e.g., in uranyl *nitrate*, $UO_2(NO_3)_2$) is 5 Å[32] which is closer to the O–O distance between the phosphates in the minor groove (7–11 Å, sequence dependent), whereas the O–O distance in the major groove is considerably larger (∼14 Å) (e.g., in the crystal structure of the Drew–Dickerson dodecamer[33]). Indeed, uranyl binding in the DNA minor groove is consistent with recent photocleavage results which show that uranyl photocleavage of DNA—in acetate buffer at pH 6.5—is preferentially taking place from the minor groove and especially at positions where the minor groove is predicted to be most narrow.[10] Some uranyl bridging between DNA molecules also occurs as evidenced by the aggregation observed by LD (Figure 3). Under some conditions (e.g., as pH is raised), it is very likely that multinuclear uranyl species bind to the DNA and are responsible for the photocleavage.

DNA Photocleavage. The linear dichroism results show that uranyl binding to the DNA is a prerequisite for photocleavage, and the plasmid relaxation results show that photocleavage is not inhibited by a radical quencher (glycerol). These observations provide strong support to our previous suggestion[7] that photocleavage does not involve diffusing species, such as hydroxyl radicals. Indeed, our results using methylphosphonate containing oligonucleotides as substrates show that photocleavage is taking place proximal to the phosphate to which the uranyl is bound. These results, furthermore, allow us to conclude that the probability of photocleavage at the 3′-side is equal to that at the 5′-side of the phosphate. Recently, evidence has also been presented showing that uranyl has relatively increased affinity for phosphate monoesters, e.g., 3′- and especially 5′-terminal phosphate groups of oligonucleotides, and thus preferentially cleave there at very low uranyl concentrations (1–10 µM) and in the presence of a chelator.[34] We observed no such effect under the conditions used for the present experiments.

Although the photophysics of the UO_2^{2+} ion has been studied extensively, the identity of the excited species is still a matter of some controversy[35] (and is only of minor importance in the present context). It is well documented, however, that the excited uranyl(VI) ion (UO_2^{2+})*, is a strong oxidant,[36] capable of oxidizing, e.g., alcohols[37,38] and olefins[39] to carbonyl compounds in aqueous solution. The mechanism of these photooxidations is not fully elucidated, but a hydrogen abstraction step is almost certainly involved,[38] and in the case of oxidation of alcohols, it has been proposed that homolytic splitting of H_2O molecules in the hydration shell of the UO_2^{2+} ion takes place thereby generating hydroxyl radicals locally:

$$[O_2U^{VI}(H_2O)_n]^{2+} \xrightarrow{h\vartheta} {}^*[O_2U^{VI}(H_2O)_n]^{2+} \rightarrow$$
$$[(H_2O)_{n-1}(O_2U^V-H^{\bullet}){}^{\bullet}OH]^{2+}$$
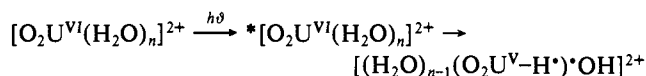
This mechanism could also be operational for uranyl bound to DNA since these locally produced hydroxyl radicals may in turn abstract hydrogen from the nearest deoxyribose of the DNA backbone. Alternatively or additionally, the UO_2^{2+} ions bound to the DNA phosphates may directly abstract hydrogen from the deoxyribose.

The 1′, 3′, 4′, and 5′ positions of the deoxyribose moiety are activated for hydrogen abstraction, and attacks at the 1′, 3′, and 4′ position have previously been implied in the DNA cleavage by other metal complexes such as bleomycin (Fe^{II})[40] and phenanthroline₂ (CuI).[41] Structurally, the 1′, 4′, and 5′ hydrogens are mainly accessible from the minor groove in B-DNA, whereas the 3′-hydrogen is more accessible from the major groove. Since the uranyl-mediated photocleavage of DNA does not involve alkaline sensitive sites and is apparently not dependent on O_2, the predominant reaction resembles that of phenanthroline₂(CuI), i.e., attack at 1′ position, from the minor groove. However, as observed both by HPLC and gel electrophoretic analysis more than one product is formed and thus more than one pathway is likely. Further experiments are in progress to resolve the mechanism.

(32) Dalley, N. K.; Mueller, M. H.; Simonsen, S. H. *Inorg. Chem.* **1971**, *10*, 323–328.

(33) Wing, R.; Drew, H.; Takano, T.; Broka, C.; Tanaka, S.; Itakura, K.; Dickerson, R. E. *Nature* **1980**, *282*, 755–758.

(34) Aubrey, R. H., Jr.; Orgel, L. E. *Bioconjugate Chem.* **1991**, *2*, 431–434.

(35) Marcantonatos, M. D.; Pawlowska, M. M. *J. Chem. Soc., Faraday Trans.* **1989**, *85*, 2481–2498.

(36) Burrows, H. D.; Kemp, T. J. *Chem. Soc. Rev.* **1974**, *3*, 138–165.

(37) Azenha, M. E. D. G.; Burrows, H. D.; Furmosinho, S. J.; Miguel, M. G. M. *J. Chem. Soc., Faraday Trans.* **1989**, *85*, 2625–2634.

(38) Cunningham, J.; Srijaranai, S. *J. Photochem. Photobiol. A. Chem.* **1990**, *55*, 219–232.

(39) Murayama, E.; Sato, T. *Bull. Chem. Soc. Japan* **1978**, *51*, 3022–3026.

(40) Rabow, L. E.; Stubbe, J.; Kozarich, J. W. *J. Am. Chem. Soc.* **1990**, *112*, 3196–3203. Rabow, L. E.; McGall, G. H.; Stubbe, J.; Kozarich, J. W. *J. Am. Chem. Soc.* **1990**, *112*, 3203–3208.

(41) Stubbe, J.; Kozarich, J. W. *Chem. Rev.* **1987**, *87*, 1107–1136. Goyne, T. E.; Sigman, D. S. *J. Am. Chem. Soc.* **1987**, *109*, 2846–2848.